

# **Lawrence Berkeley National Laboratory**

## Lawrence Berkeley National Laboratory

**Title**

Poroelastic modeling of seismic boundary conditions across a fracture

**Permalink**

<https://escholarship.org/uc/item/96w6r5rw>

**Authors**

Schoenberg, M.A.  
Nakagawa, S.

**Publication Date**

2006-06-29

Peer reviewed

## Poroelastic modeling of seismic boundary conditions across a fracture

*M.A. Schoenberg, Consultant, 5 Mountain Rd., West Redding CT06896*

*S. Nakagawa\*, Earth Sciences Division, Lawrence Berkeley National Laboratory, Berkeley CA94720*

### Summary

A fracture within a porous background is modeled as a thin porous layer with increased compliance and finite permeability. For small layer thickness, a set of boundary conditions can be derived that relate particle velocity and stress across a fracture, induced by incident poroelastic waves. These boundary conditions are given via phenomenological parameters that can be used to examine and characterize the seismic response of a fracture. One of these parameters, here it is called membrane permeability, is shown through several examples to control the scattering amplitude of the slow P waves for very low-permeability fractures, which in turn controls the intrinsic attenuation of the waves.

### Introduction

Sedimentary rock is often permeated by fractures, fault and joints occurring in sets with a common alignment. When background permeability is small, the degree of fracturing, the physical nature of the fractures, and their orientation, are vital data for understanding the fluid flow in rocks.

In non-permeable media, specifying how the elastic moduli of a layer approach zero as the cumulative thickness of the layer approaches zero yields a set of phenomenological parameters which describe the additional compliance of the equivalent medium due to the presence of fractures (Schoenberg, 1980). The relation between acoustics and flow in permeable media has been described successfully by Biot theory, and this same approach will be used to derive the acoustic behavior of fractures in permeable rocks.

In permeable media, a fracture may also be treated as a thin layer. Associated with it is a set P of parameters specifying the elastic and flow properties of the layer as a function of the layer thickness. As in the case of non-permeable layers, natural boundary conditions (open pores for the flow condition, no displacement discontinuities at the layer boundaries) are applied. Then allowing the thickness to approach zero leaves a subset  $P_0$  of the parameter set which specifies, by way of the actual boundary conditions across the fracture, the average behavior of the fracture. It is still an open question whether such a surface may be sounded in a way that allows the parameters of  $P_0$  which control the flow in the fracture to be estimated.

### Theory

Our objective is to derive a set of boundary conditions for a thin poroelastic layer embedded within a homogeneous isotropic background poroelastic medium. The governing equations of poroelastic wave propagation can be stated as

$$\begin{aligned} \boldsymbol{\tau} &= G(\nabla \mathbf{u} + \mathbf{u} \nabla) + [(K_U - 2G/3)\nabla \cdot \mathbf{u} + C\nabla \cdot \mathbf{w}] \mathbf{I} \\ -p_f &= C\nabla \cdot \mathbf{u} + M\nabla \cdot \mathbf{w} \\ \nabla \cdot \boldsymbol{\tau} &= -\omega^2 (\rho \mathbf{u} + \rho_f \mathbf{w}) \\ -\nabla p_f &= -\omega^2 (\rho_f \mathbf{u} + \tilde{\rho} \mathbf{w}), \tilde{\rho} \equiv i\eta_f / \omega k(\omega) \end{aligned} \quad (1)$$

where  $\mathbf{u}$  is the local average solid frame displacement,  $\mathbf{w} = \phi (\mathbf{U} - \mathbf{u})$  is the relative fluid volume displacement defined via  $\mathbf{u}$ , local fluid displacement in the pore space  $\mathbf{U}$  and porosity  $\phi$ .  $\boldsymbol{\tau}$  is the total stress and  $p_f$  is the fluid pressure.  $G$  is the frame shear modulus and  $K_U$  is the undrained bulk modulus.  $\rho$  is the bulk density,  $\rho_f$  is the fluid modulus, and the parameter  $\tilde{\rho}$  is defined via fluid viscosity  $\eta_f$  and the frequency-dependent permeability  $k(\omega)$  (e.g., Johnson et al., 1987). Definitions of  $C$  and  $M$  and their relationships to other parameters can be found in standard poroelasticity literature (e.g., Pride, 2003). Solving these equations assuming a plane harmonic wave field results in four plane waves (fast and slow P waves and two S waves).

Consider an interface across which certain stress and displacement (velocity) components are conserved. We assume this interface to be normal to the 3<sup>rd</sup> direction and the wave propagation parallel to the 1, 3 plane. For a homogeneous medium, we can assume a plane harmonic wave field proportional to  $\exp i\omega(\xi_1 x_1 - t)$ . The plane wave displacement and stress are introduced into Eqs.(1). With substitutions  $\partial/\partial x_1 \rightarrow i\omega\xi_1$  and  $\partial/\partial x_2 \rightarrow 0$  and by eliminating variables that can be discontinuous across the interface, the following coupled first-order differential equations are derived (Note: in this paper, an uncoupled shear wave with out-of-plane motions is not discussed)

$$\frac{\partial}{\partial x_3} \begin{bmatrix} \dot{u}_1 \\ \tau_{33} \\ -p_f \\ \tau_{13} \\ \dot{u}_3 \\ \dot{w}_3 \end{bmatrix} = -i\omega \begin{bmatrix} \mathbf{0} & \mathbf{Q}_{XY} \\ \mathbf{Q}_{YX} & \mathbf{0} \end{bmatrix} \begin{bmatrix} \dot{u}_1 \\ \tau_{33} \\ -p_f \\ \tau_{13} \\ \dot{u}_3 \\ \dot{w}_3 \end{bmatrix}, \quad (2)$$

## Seismic boundary conditions for fractures in poroelastic media

where the submatrices are defined as

$$\mathbf{Q}_{XY} \equiv \begin{bmatrix} 1/G & \xi_1 & 0 \\ \xi_1 & \rho & \rho_f \\ 0 & \rho_f & \tilde{\rho} \end{bmatrix}, \quad (3)$$

$$\mathbf{Q}_{YX} \equiv \begin{bmatrix} -4G\xi_1^2 \left(1 + \frac{2}{3} \frac{G}{H_D}\right) - \frac{\rho_f^2 - \rho\tilde{\rho}}{\tilde{\rho}} & \xi_1 \left(1 - \frac{2G}{H_D}\right) & \xi_1 \left(-\frac{\rho_f}{\tilde{\rho}} + \alpha \frac{2G}{H_D}\right) \\ \xi_1 \left(1 - \frac{2G}{H_D}\right) & \frac{1}{H_D} & -\frac{\alpha}{H_D} \\ \xi_1 \left(-\frac{\rho_f}{\tilde{\rho}} + \alpha \frac{2G}{H_D}\right) & -\frac{\alpha}{H_D} & \frac{\alpha^2}{H_D} + \frac{1}{M} - \frac{\xi_1^2}{\tilde{\rho}} \end{bmatrix}, \quad (4)$$

where  $\alpha = (1-K_D/K_U)/B$  and  $H_D = K_D + 4G/3$ .  $K_D$  is the drained (dry) bulk modulus and  $B$  is the Skempton's  $B$  coefficient. Assuming homogeneous material properties, both sides of Eq.(2) can be integrated over the thickness  $h$  of the layer (fracture) located around  $x_3=0$  to obtain

$$\begin{bmatrix} \dot{u}_1 \\ \tau_{33} \\ -p_f \\ \tau_{13} \\ \dot{u}_3 \\ \dot{w}_3 \end{bmatrix}_{x_3=\frac{h}{2}} - \begin{bmatrix} \dot{u}_1 \\ \tau_{33} \\ -p_f \\ \tau_{13} \\ \dot{u}_3 \\ \dot{w}_3 \end{bmatrix}_{x_3=-\frac{h}{2}} = -i\omega h \begin{bmatrix} \mathbf{0} & \mathbf{Q}_{XY} \\ \mathbf{Q}_{YX} & \mathbf{0} \end{bmatrix} \begin{bmatrix} \bar{u}_1 \\ \bar{\tau}_{33} \\ -\bar{p}_f \\ \bar{\tau}_{13} \\ \bar{u}_3 \\ \bar{w}_3 \end{bmatrix}. \quad (5)$$

The vector on the right hand side contains an average of the variables across the thickness of the layer representing a fracture.

For a fracture thickness  $h$  that is much smaller than the wavelength, many components of the matrices  $h\mathbf{Q}_{XY}$  and  $h\mathbf{Q}_{YX}$  can be negligibly small. However, by defining parameters that result in non-vanishing components in the coefficient matrices, the behavior of a fracture with an unknown thickness can be examined, analogously to the way parameters are defined and used for the linear-slip interface conditions for elastic and viscoelastic fractures (Schoenberg, 1980). These parameters are

$$\begin{aligned} \eta_{N_D} &\equiv h/H_D : \text{Dry normal fracture compliance} \\ \eta_T &\equiv h/G : \text{Shear fracture compliance} \\ \eta_{N_U} &\equiv h/H_U : \text{Undrained normal fracture compliance} \\ \hat{\kappa}(\omega) &\equiv k(\omega)/h : \text{Membrane (or interface) permeability} \end{aligned}$$

$H_U$  is the undrained P-wave modulus defined by  $H=K_U+4G/3$ . It is noted that for very large fracture permeability, terms proportional to  $h/\tilde{\rho}=h\omega k(\omega)/i\eta_f$  in

$h\mathbf{Q}_{YX}$  can also be non-negligible. However, numerical simulations indicate that these terms produce no effect on the scattering of the waves and can be neglected.

Using these parameters, a set of boundary conditions for a compliant fracture is obtained as

$$\begin{aligned} [\tau_{13}] &= 0 \\ [\tau_{33}] &= 0 \\ [-p_f] &= (\eta_f / \kappa_{brane}) \bar{w}_3 \\ [\dot{u}_1] &= -i\omega \eta_T \tau_{13} \\ [\dot{u}_3] &= -i\omega \eta_{N_U} (\tau_{33} - \alpha(-\bar{p}_f)) \\ [\dot{w}_3] &= -i\omega \eta_{N_D} (-\alpha) \left( \tau_{33} - \alpha \frac{\eta_{N_D}}{\eta_{N_D} - \eta_{N_U}} (-\bar{p}_f) \right) \end{aligned} \quad (6)$$

For continuous variables (with a jump across a fracture  $[\cdot]=0$ ), no distinction is made between the values on the boundary and the averaged quantity. The third equation is the manifestation of Darcy's law for a thin layer (Gurevich and Schoenberg, 1999), and the last two equations give the one dimensional description of stress partitioning within a poroelastic medium, including the effective stress law.

For highly permeable (or open) fractures,  $\hat{\kappa}(\omega)$  becomes large and the right hand side of the third equation can be ignored. This allows us to separate the stress variables that are continuous across the fracture and the velocity (or displacement) variables that are discontinuous across the fracture, which results in a set of very simple boundary conditions similar to the original linear slip interface conditions.

In contrast, for low-permeability (or clogged) fractures, the unknown distribution of the variables across the fracture needs to be found through the boundary values, e.g.,  $p_f^+ = p_f(x_3=h/2)$  and  $p_f^- = p_f(x_3=-h/2)$ , to completely define the boundary conditions in Eqs.(6). The simplest approach is to express the average of the field via an average of the two boundary values, e.g.,  $\bar{p}_f = (p_f^+ + p_f^-)/2$ , or, equivalently, to assume linear changes in the field. This averaging scheme can be extended to include directly in Eq.(5) all the terms in the  $\mathbf{Q}_{XY}$  and  $\mathbf{Q}_{YX}$ , that were neglected for small  $hs$ . For predicting the behavior of slow P waves, however, this approximation can be inaccurate as shown in the following examples.

### Examples

In the first example, boundary conditions for a poroelastic fracture are used to compute plane wave scattering and the results are compared to the prediction of a numerical code based on the Kennett's algorithm (Kennett, 1983) using

## Seismic boundary conditions for fractures in poroelastic media

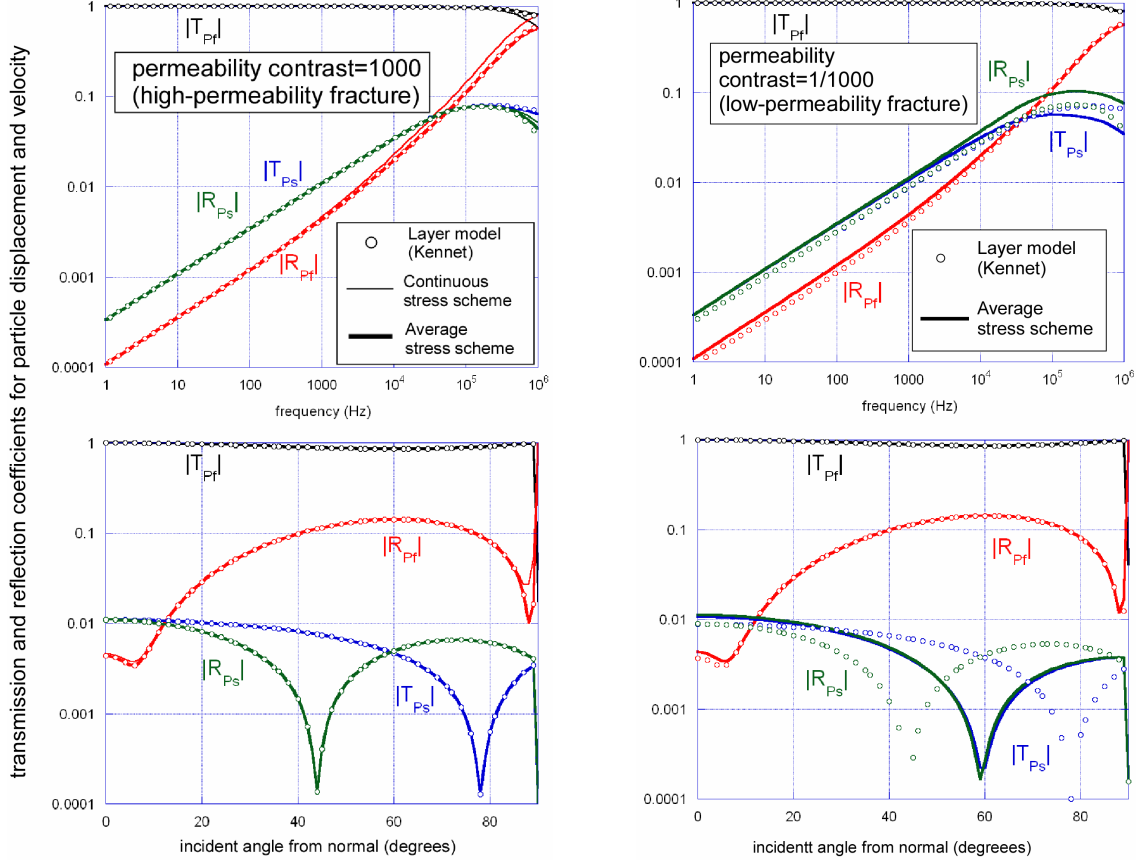


Figure 1: Comparison of the plane wave scattering amplitudes from both a layer model (“truth”) and the two fracture models. The amplitudes of transmission and reflection coefficients are shown as  $|T_{Pf}|$ ,  $|R_{Pf}|$  for fast P waves, and  $|T_{Ps}|$ ,  $|R_{Ps}|$  for slow P waves, respectively, for incident fast P waves.

equivalent material properties for the center layer representing a fracture, surrounded by half-spaces. In this paper, we focus on the scattering amplitude of incoming fast P waves converted into fast and slow P waves, based on solid frame displacement (or velocity).

For a set of background material properties considered “typical” for high-permeability sandstone with a permeability of  $10^{-15} \text{ m}^2$  (100 md) and a saturated, compliant fracture (dry compliances  $\eta_{N_p} = 1 \times 10^{-9} \text{ m/Pa}$  and  $\eta_T = 3 \times 10^{-9} \text{ m/Pa}$ ) with a thickness  $h=1 \text{ mm}$ , either the frequency of the incoming waves or the angle of incidence for the incoming fast P wave is varied. In Fig.1, amplitude vs. frequency (top) is shown for normal incidence, and the incidence angle vs. amplitude (bottom) is shown for a frequency of 1 kHz. The low-frequency results of the three models agree well for a high-permeability fracture (Left column of Fig.1: fracture permeability/background permeability = 1000). In contrast, significant disagreement is present for a low-permeability fracture (Right column of

Fig.1: the permeability ratio=1/1000) using the “averaging scheme” model. For this case, the “continuous stress scheme” model was not used because of the expected finite jump in the pressure across a fracture.

In the second example, the same material properties as in the first example are used. In this case, only the layer model was used to examine if the membrane permeability could still have any physical significance even when the fracture models did not perform well for very low fracture permeability. For five values of static membrane permeability  $\hat{K}(0)$ , the fracture (layer) thickness was varied from 1 cm to 1  $\mu\text{m}$ , and the fracture permeability was altered accordingly (Fig.2). The results showed that all curves with a common  $\hat{K}(0)$  collapsed onto single curves below 10 kHz (For lower  $\hat{K}(0)$ ’s, two curves are present for both transmission and reflection coefficients of the slow P waves), which indicates that  $\hat{K}$  can be one of the controlling factors to determine the scattering of slow P waves.

## Seismic boundary conditions for fractures in poroelastic media

### Conclusions

A set of boundary conditions can be derived for a compliant fracture modeled as a thin poroelastic layer embedded in a poroelastic background.

For high-permeability fractures, the boundary conditions consist of stress continuity conditions and velocity discontinuity conditions (same as the linear-slip interface conditions for elastic and viscoelastic fractures). The scattering of waves computed by this model agrees well with the layer model, which provided the “ground truth”.

For low-permeability (clogged) fractures, both fluid velocity and pressure can be discontinuous across the fracture. We attempted to solve this problem by approximating the velocity and pressure field using a linear function determined by known variables on the surfaces of a fracture, which slightly improved the prediction for the reflection of fast P waves at high frequencies (Fig.1). However, the error for the scattering of slow P waves increased with decreasing permeability of the fracture. The (static) membrane permeability defined via the fracture models, however, still plays a significant role in affecting the slow P wave scattering for very small fracture permeability.

The discrepancies between the results from the layer model and the “average scheme” model may be caused by the errors in evaluating the average fluid pressure and velocity inside the fracture. Within a compliant low-permeability fracture, if the excess pressure building up during a passage of wave cannot diffuse into the surrounding medium, the resulting fluid pressure and velocity distribution may not be well approximated by a linear function (Fig.3). In the future research, the diffusion of fluid pressure within the fracture will be considered explicitly in the derivation of improved boundary conditions.

### References

- Gurevich, B. and Schoenberg, M.A., 1999, Interface conditions for Biot’s equation of poroelasticity, *J. Acoust. Soc. Am.*, 105, 2585-2589.
- Johnson, D.L., Koplik, J. and Dashen, R., 1987, Theory of dynamic permeability and tortuosity in fluid-saturated porous media, *J. Fluid Mech.*, 176, 379-402.
- Kennett, B.L.N., 1983, *Seismic Wave Propagation in Stratified Media*, Cambridge Univ. Press, New York.
- Pride, S.R., 2003, Relationships between seismic and hydrological properties, in *Hydrogeophysics*, edit. Y. Rubin and S. Hubbard, 1-31, Kluwer Acad., New York.

Schoenberg, M., 1980, Elastic wave behavior across linear slip interfaces, *J. Acoust. Soc. Am.*, 68, 1516-1521.

### Acknowledgments

This research has been supported by the Office of Science, Office of Basic Energy Sciences, Division of Chemical Sciences of the U.S. Department of Energy under contract No. DE-AC76SF00098. Michael Schoenberg would like to express appreciation to Patrick Rasolofosaon of IFP and David Johnson and Robert Burridge while at Schlumberger for suggestions and discussions on poroelasticity of fractures. Both authors would like to thank Steven Pride at LBNL for his help in more recent development of the theory and providing physical insights into the theory of poroelastic waves.

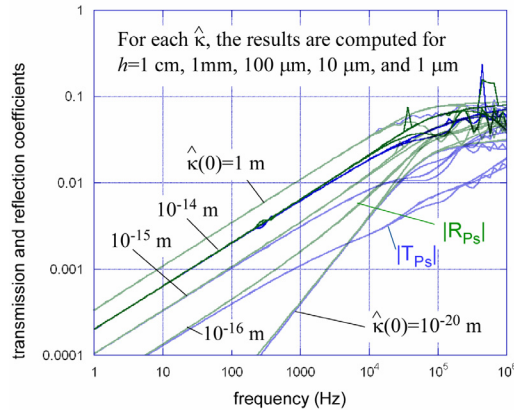


Figure 2: Transmission and reflection coefficients of slow P waves for a range of static membrane permeability.

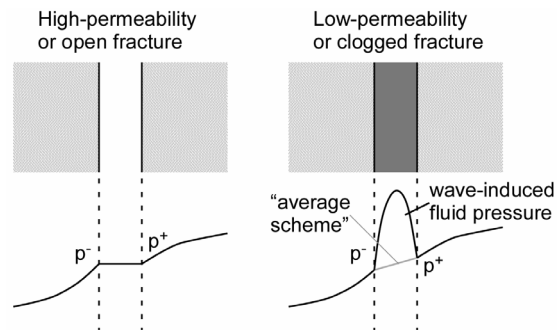


Figure 3: For a high permeability fracture, the fluid pressure across the fracture is continuous, which can be well approximated by either continuous or linear (average) model. For low permeability fracture, however, the elevated fluid pressure within the fracture induced by waves, which does not have enough time to diffuse out, is not captured by a linear function.